Microstructural investigation of as-deposited Co-Ag nano-granular films

1995 J. Phys.: Condens. Matter 7 9425

(http://iopscience.iop.org/0953-8984/7/49/007)

J. Phys.: Condens. Matter 7 (1995) 9425–9432. Printed in the UK

Microstructural investigation of as-deposited Co–Ag nano-granular films

J H Du, Q Li, L C Wang, H Sang, S Y Zhang, Y W Du and D Feng

Laboratory of Solid State Microstructures and Centre for Advanced Studies in Science and Technology of Microstructures, Nanjing University, Nanjing 210093, People's Republic of China

Received 10 April 1995

Abstract. The microstructures of as-deposited Co–Ag nano-granular films are characterized by x-ray diffraction, transmission electron microscopy and high-resolution electron microscopy. In as-deposited films, there is a strong tendency for phase separation to occur; Co and Ag particles coexist in the films. The average size of Co grains varies with the Co concentration. Ag particles have the preferential lattice orientation ⟨110⟩ and Co particles have lattice orientations ⟨110⟩, ⟨111⟩, ⟨112⟩, and ⟨100⟩ in the direction of the film surface normal. There is a tendency for two connecting grains to have two groups of parallel lattice planes.

1. Introduction

Since the discovery of giant magnetoresistance (GMR) at room temperature in Co/Cu antiferromagnetically coupled multilayers [1, 2], it has also been found in granular Co–Cu, Fe–Ag and Co–Ag films, for example [3–8]. These systems stimulate great interest since they have prominent merit as regards potential commercial application: their magnetoresistance amplitudes may be larger than in multilayers in the usual CIP geometry; they are also simpler to prepare and have good thermal stability after annealing. The GMR behaviour of such films has been demonstrated to be closely related to structural features, such as the sizes of the magnetic grains, their separations, and the roughness of the interface between the magnetic grains and the matrix. Precise microstructural information about granular films is important for establishing a GMR model.

These film samples are usually obtained by codepositing on a substrate two immiscible metallic components, one magnetic, and the other nonmagnetic (e.g. Co and Ag). Because of their immiscibility, the two metallic components tend to segregate resulting in the formation of small magnetic precipitates embedded in a nonmagnetic matrix. However, as a nonequilibrium process, sputtering onto a substrate at low temperature can readily lead to formation of metastable alloys [9]. During deposition, the two tendencies coexist and compete, and the microstructures of the as-deposited films are dictated by the degree of immiscibility of the two metals and the substrate temperature during deposition. Investigations by x-ray diffraction of the microstructures of the films deposited onto a substrate at room temperature, such as the Co–Cu and NiFe–Ag systems, have suggested the presence of magnetic particles accompanying alloying between the two components [4, 12]. For Co–Ag and Fe–Ag systems, intensive investigation has recently been carried out by Li *et al* by atomic resolution and nanochemical analysis electron microscopy [10]. Their results suggested the presence of Co clusters—but poorly crystallized with sizes less than

0953-8984/95/499425+08$19.50

1.5 nm. However, the films they investigated were too thin to be continuous, and structural investigation of such films cannot be compared to other measurements of properties made on continuous films. In contrast, the Co–Ag films we study are continuous with deposition thicknesses of about 400 nm, and the results are somewhat different. In this paper, we report the investigation of as-deposited Co–Ag granular film samples by x-ray diffraction (XRD), transmission electron microscopy (TEM) and high-resolution electron microscopy (HREM).

2. Experimental procedure

Co–Ag granular film samples were prepared using an ion-beam cosputtering technique. The sputtering chamber with high vacuum is equipped with a Kauffman ion gun in which the argon (99.99%) pressure is 26 mPa. An argon-ion beam with energy 1.2 keV was employed during deposition. The targets consisted of pure silver and cobalt with small pieces of cobalt adhering to the plate of silver. By adjusting the number of pieces of cobalt, the cobalt concentration of the film samples could be varied. A series of film samples with different cobalt concentrations were deposited onto glass substrates and also on pyroxylin colloid-coated copper grids placed on them for preparing electron microscopy specimens. Both the substrates and the targets were water cooled to maintain the temperature at room temperature (300 K). The thicknesses of these films were about 400 nm. Subsequently these films were removed from the substrates to undergo composition measurements via electron microprobe analysis, characterization by x-ray diffraction, and magnetoresistance measurements. The conventional four-terminal method was employed to measure the GMR values of these samples in an applied magnetic field of up to 11.2 kOe. The film on the copper grids was ion thinned by using a GATAN DUAL ION MILL 600 with a 1 mA ion beam current under an accelerating voltage of 4 kV. The time required was several minutes; then the electron microscopy specimen was obtained. Electron microscopy observations were made with a JEM-4000EX high-resolution electron microscope (spherical aberration coefficient $C_s = 1.0$ mm) operated at an accelerating voltage of 300 keV.

3. Results and discussion

A series of as-deposited Co_xAg_{1-x} granular film samples were fabricated with concentrations ranging from $x = 8$ to $x = 40$ at.%. The GMR results for these samples are shown in figure 1. The structures of these films were first investigated by x-ray diffraction. Figure 2 shows XRD patterns of these film samples. These patterns show peaks attributable to Ag(111), Ag(200)[Co(111)], Ag(220), and Ag(311) diffractions. As cobalt concentration increases, the Ag(111) peak is barely shifted, indicating that the tendency of CoAg to alloy within the Ag matrix is weak, and that Co atoms segregate, resulting in the formation of Co grains. Because CoAg alloying will lead to a reduction of Ag(111) lattice spacing, there is a shift to the right of the Ag(111) peak. The second peaks in these patterns are attributable to both Ag(200) and Co(111) diffractions. From the evolution tendency of the three Ag peaks with cobalt concentration, one tends to infer that the proportion of Ag(200) peak in the second peak gradually decreases until it nearly vanishes at high cobalt concentration. In contrast, the proportion of Co(111) peak gradually increases with the increase of the cobalt concentration, resulting in a continuous increase of the second peaks at high cobalt concentration. For these samples, a Co(111) peak is clearly visible at high cobalt concentration (33 at.%, 40 at.%) but merges into the Ag(200) peak in the second peak at low cobalt concentration.

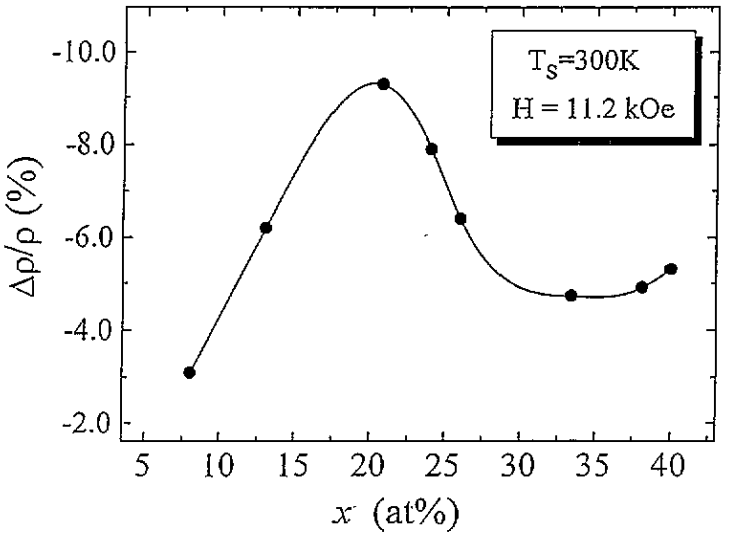

Figure 1. The MR ratio $\Delta\rho/\rho$ measured at room temperature as a function of cobalt concentration x for Co_xAg_{1-x} samples prepared at a substrate temperature of $T_s = 300$ K.

Moreover, the Co(111) peak in the pattern for 40 at.% cobalt concentration shifts to the left by about 0.8° from the bulk Co(200) peak. This suggests that Ag atoms form alloys with Co atoms within Co particles, and that demixing of Co and Ag in the Co particles is not thorough. Because CoAg alloying will cause an increase of the Co(111) lattice spacing, the shift to the left of the bulk Co(111) peak is expected. Finally, the extra-strong Ag(111) peaks shown by these patterns reveal highly ⟨111⟩-textured films; in addition, the fact that peaks of Ag(111), Ag(200), Ag(220), and Ag(311) diffraction occur together indicates that the Ag grains of these films possess preferential ⟨110⟩ lattice orientation in the direction of the film surface normal.

The XRD technique studies the overall area of a film. In contrast, TEM can investigate a microscopic area. $Co_{22}Ag_{78}$ and $Co_{40}Ag_{60}$ samples were also studied by TEM. Special areas rich in Co particles in the two films were selected and investigated. Selected-area electron diffraction (SAED) patterns of the two films are shown in figures 3(a) and 3(b) respectively. In the SAED patterns the first three rings correspond to Ag(111), Ag(200)[Co(111)], and Co(200) diffraction respectively. The intensity of Ag(111) diffraction is too weak to be seen, indicating that the intensity of Ag(200) diffraction is negligible and that the second ring is almost entirely due to Co(111) diffraction. Thus dark-field images showing only Co particles can be recorded by including part of the second and third rings in the objective lens aperture, as illustrated in figures 3(c) and 3(d). It is clearly seen that the average size of Co grains in the $Co_{22}Ag_{78}$ sample is less than that in the $Co_{40}Ag_{60}$ sample, and the distribution of Co grains in the $Co_{22}Ag_{78}$ sample is denser than that in the $Co_{40}Ag_{78}$ sample.

The above results are consistent with the conclusions about GMR behaviour of granular films reached so far: GMR is lacking in homogeneous ferromagnetic alloys and occurs in inhomogeneous magnetic media containing nonaligned ferromagnetic entities on a microscopic length scale—roughly that of the mean free path (Λ); within Λ (of the order of a few hundred Å as estimated from resistivity) the scattering events due to nonaligned magnetic particles contribute to the GMR; the magnitude of the GMR is dictated by the average size and the number of the magnetic particles within Λ; and the GMR scales

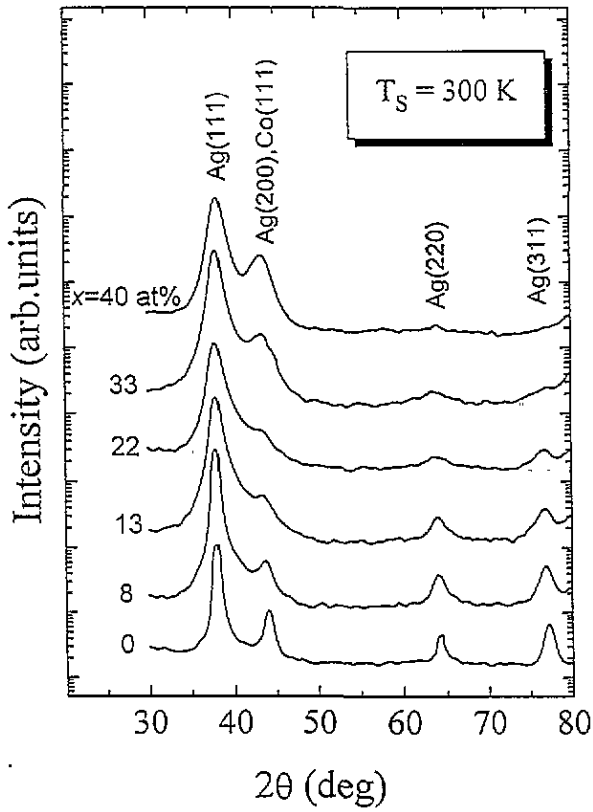

Figure 2. XRD patterns for six as-deposited Co–Ag film samples (T_s = 300 K) with different cobalt concentrations, with a logarithmically scaled ordinate axis.

inversely with the average magnetic grain diameter. The tendency towards Co and Ag phase separation results in GMR behaviour in CoAg films. When the cobalt concentration is lower (8 at.%, 13 at.%, 22 at.%), Co grains are small and the size variation of Co grains with cobalt concentration is not obvious; thus the number of Co grains within Λ increases with cobalt concentration, so the GMR value increases with cobalt concentration. When the cobalt concentration increases continuously, the average size of Co grains increases and the number of Co grains within Λ becomes lower; this leads to a decrease of the GMR. Thus, as shown in figure 1, 22% cobalt concentration is a turning point, with the optimal GMR value among those for this series of samples. However, the GMR of the as-deposited $Co_{22}Ag_{78}$ film is increased from 9% to 13.4% after annealing for half an hour at 500 K [11]. Post-annealing treatment made the sizes of Co grains slightly larger and led to progressive demixing of Ag and Co, so the GMR depends not only on the size and distribution of Co grains, but also on other factors, such as roughness of the interface between Co grains and the matrix. HREM is a strong tool for obtaining precise microstructural information. Below we give the results for the as-deposited $Co_{22}Ag_{78}$ film obtained by HREM; the investigations of the post-anneal films by HREM will be reported elsewhere.

A $Co_{22}Ag_{78}$ sample was investigated by HREM. The HREM observations require a foil thickness of several tens of nm for optimal lattice imaging and to prevent overlapping of grains in the image. Such areas are encountered at the peripheries of the hole or splits in the HREM foil, where the Co–Ag granular films are supported on the pyroxylin colloid

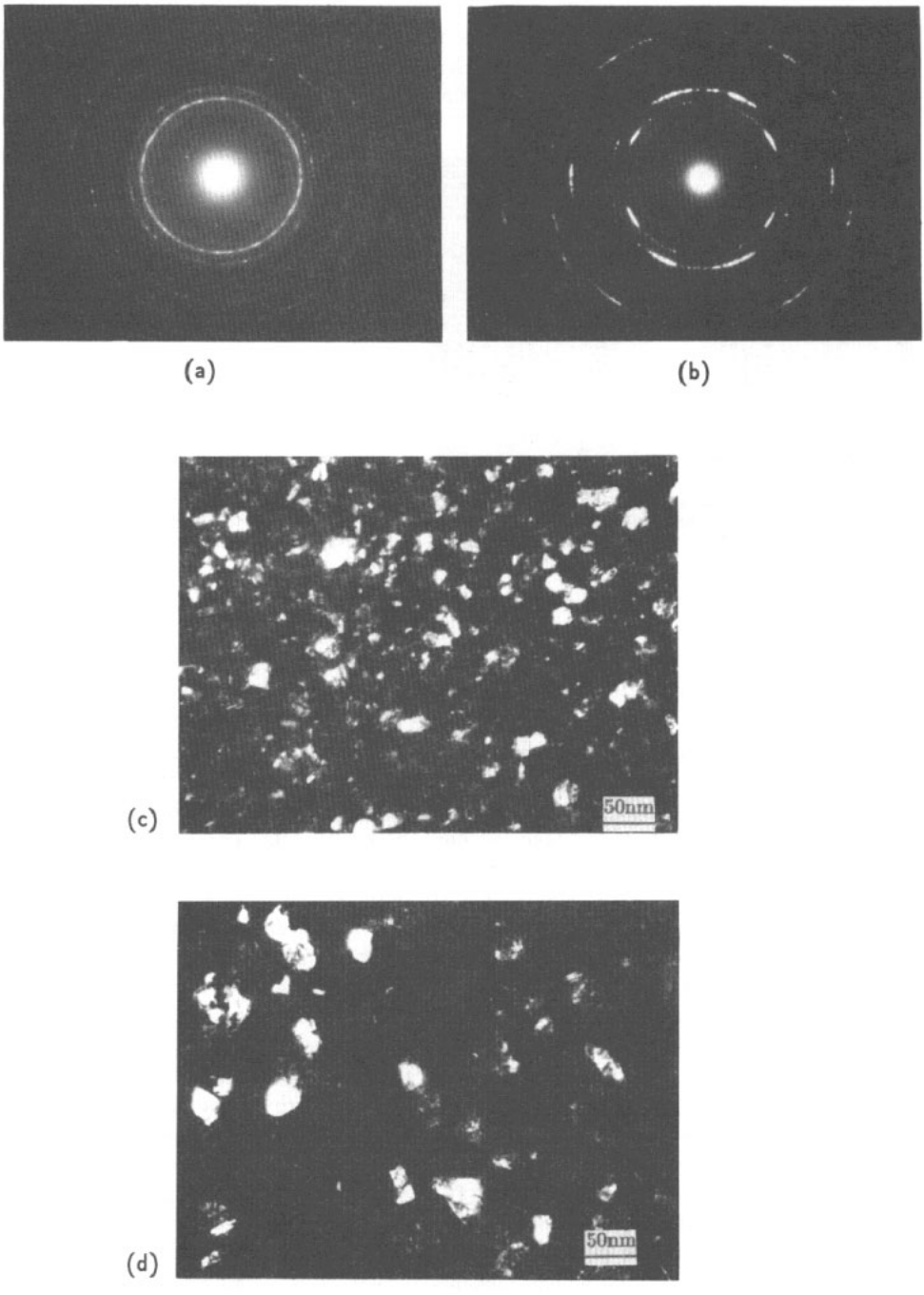

Figure 3. SAED patterns and TEM images of $Co_{22}Ag_{78}$ and $Co_{40}Ag_{60}$ films. (a) and (c) show the SAED pattern and TEM image of the $Co_{22}Ag_{78}$ film, while (b) and (d) show the SAED pattern and TEM image of the $Co_{40}Ag_{60}$ film.

films, and the contrast between them can be clearly seen. During HREM observations, it was noticed that at the borders of the Co–Ag granular films there was not the amorphous region usually seen for other ion-thinned HREM foils. This indicates that effects on the samples caused by ion thinning are negligible.

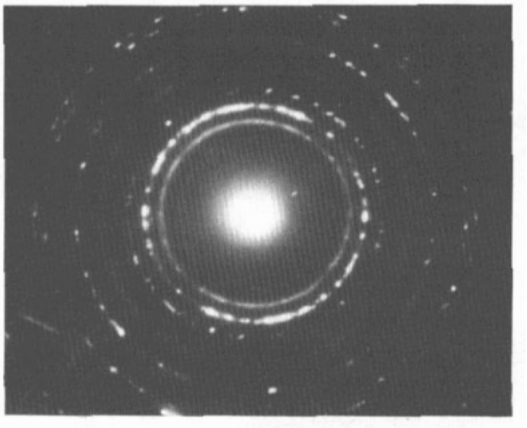

Figure 4. The SAED pattern of an as-deposited $Co_{22}Ag_{78}$ film.

Figure 4 shows a SAED pattern corresponding to the region imaged by high-resolution electron microscopy. Two sets of f.c.c. polycrystalline diffraction rings exist in the SAED pattern, suggesting that Ag and Co grains coexist in the area.

Different areas of the HREM foil were observed under low magnification and diffraction contrast between particles, and pyroxylin colloid formed in the bright field in these areas. It is found that the film is formed by heaping of crystalline particles. Particles connect, and some are superimposed in the film growth direction, while some are separated by voids. The sizes and shapes of the particles are quite widely distributed. The sizes of particle range from several nm to more than 20 nm. Some particles are elongated and sharp, while some are smooth like cobblestones. When the magnification is increased and clear high-resolution electron microscopic images are observed, areas of voids form amorphous contrast due to the existence of pyroxylin colloid film. The existence of pyroxylin colloid film has some influence on the imaging of grains. Only grains with suitable thickness can be clearly imaged and are not disturbed by the amorphous contrast formed by pyroxylin colloid. Thinner grains would merge in the amorphous contrast of pyroxylin colloid films and are hard to distinguish, while thicker grains themselves cannot form HREM images. Figure 5 shows the HREM image of one area of the film. We find that the film is compact. Voids rather seldom appear. Grains connect closely with narrow grain or phase boundaries.

Over the whole observed area many parts are two-dimensionally imaged. This illustrates that even if the growth is with amorphous pyroxylin colloid substrate, a preferential orientation is still obvious. The lattice distortion in grains is large. Usually within a grain, some region has a clear two-dimensional HREM lattice image, while other regions only form one-dimensional lattice plane fringes. In most cases the lattice planes near the grain boundary are slightly distorted which indicates local stresses in the grain boundary region. The atomic arrangement near grain boundaries, especially in the case of small grains, is slightly disordered.

Imaging of lattice planes is essential for distinguishing Co-rich grains from Ag-rich grains. In the granular Co–Ag film, the Co and Ag phases both have f.c.c. structure with lattice parameters of 3.5447 Å and 4.0862 Å, respectively. The spacings of Ag(111),

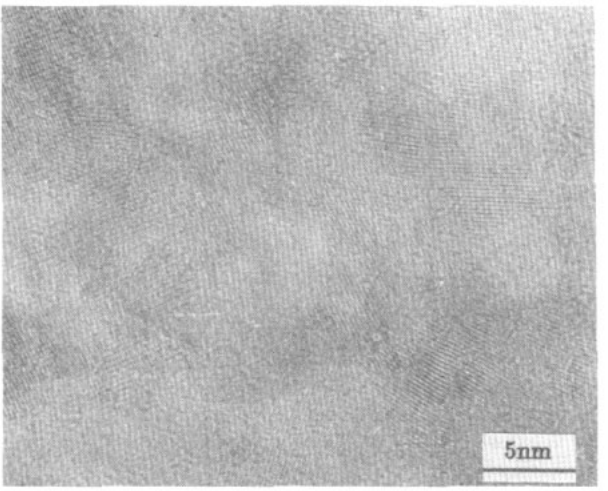

Figure 5. A high-resolution electron microscopic image of $Co_{22}Ag_{78}$ films.

Ag(200), Co(111), Co(200) planes lie above the resolution limit of the high-resolution electron microscope and these planes can be imaged. Individual crystalline particles having lattice spacings of 0.23 to 0.24 nm (Ag(111) lattice spacing) are definitely of Ag; particles having lattice spacings of 0.17 to 0.18 nm (Co(200) lattice spacing) are of Co. Imaging of a two-dimensional lattice is essential for determination of the lattice orientations for individual grains. By measuring the lattice spacings of two groups of planes and checking the angle between them, one grain's phase and orientation are judged. It is found that the lattice orientation, in the direction of the surface normal of the film, of Ag grains is mainly ⟨110⟩. Those of Co grains are ⟨110⟩, ⟨100⟩, ⟨112⟩, and ⟨111⟩; ⟨110⟩-oriented grains are usually bigger—their size reaching 20 nm or so—with grains with other orientations reaching only several nm. We also find that Co ⟨110⟩ grains of large size are often twinned on {111} lattice planes.

The structure of the film is rather typical of a granular solid. Fewer Co particles are interspersed among more Ag particles. Information about interfaces between Co particles and neighbouring Ag particles is crucial for establishing a GMR model. The atomic structure of grain (phase) boundaries can be determined only when the incident electron beam is parallel to the grain (phase) boundary plane and the boundary plane itself is parallel to low-index zone axes of neighbouring grains. Besides this, lattice distortion in the grains is large. These conditions are satisfied only seldom in grain (phase) boundaries. Grain (phase) boundaries in film samples occasionally fulfil such conditions and periodic structures are sometimes found. It is noticed that there is a tendency for two connecting grains to have two groups of parallel lattice planes; at the boundary, misfit dislocations are formed. An example is shown in figure 6. The lower part shows an Ag grain, and the upper part shows a Co grain. Ag {200} lattice planes are connected with Co {200} lattice planes. Because the lattice plane spacing of Co grains differs from that of Ag grains, every fifth Ag fringe connects with every sixth Co fringe at the boundary where periodic black/white contrast forms. This may be due to the local strain caused by the lattice misfit.

In summary, the microstructures of a series of granular Co–Ag films have been investigated by x-ray diffraction, TEM, and HREM. In as-deposited films, there is a strong tendency for phase separation to occur; Co and Ag particles coexist in the films. The

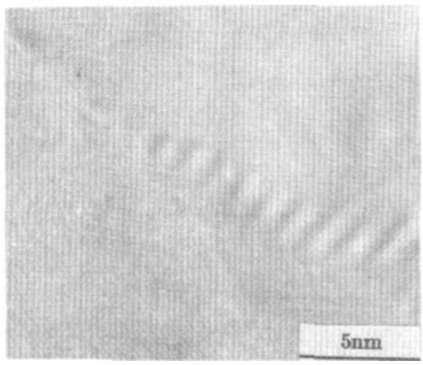

Figure 6. High-resolution electron microscopic images of the connection of Ag and Co grains. The lower part is for Ag; the upper part is for Co.

average grain size for the Co-rich case varies with the Co concentration. The sizes and shapes of the particles are quite widely distributed. Ag particles have the preferential lattice orientation ⟨110⟩ while Co particles have lattice orientations of ⟨110⟩, ⟨111⟩, ⟨112⟩, ⟨100⟩ in the direction of the film surface normal. There is a tendency for two connecting grains to have two groups of parallel lattice planes.

Acknowledgments

This work was supported by 85-6 NMS, NSFS & NAMMC, and JSNSF.

References

[1] Parkin S S P, Bhadra R and Roche K P 1991 *Phys. Rev. Lett.* **66** 2152
[2] Parkin S S P, Li Z G and Smith D J 1991 *Appl. Phys. Lett.* **58** 2710
[3] Xiao J Q, Jiang J S and Chien C L 1992 *Phys. Rev. Lett.* **68** 3749
[4] Berkowitz A E, Mitchell J R, Carey M J, Young A P, Zhang S, Spada F E, Parker F T, Hutten A and Thomas G 1992 *Phys. Rev. Lett.* **68** 3745
[5] Carey M J, Young A P, Starr A, Rao D and Berkowitz A E 1992 *Appl. Phys. Lett.* **61** 2935
[6] Xiao G, Wang J and Xiong P 1993 *Appl. Phys. Lett.* **62** 420
[7] Bernard J A, Waknis A, Tan M, Haftek E, Parker M R and Watson M L 1992 *J. Magn. Magn. Mater.* **114** L230
[8] Tsoukatos A, Wan H, Hadjipanayis G C and Li Z G 1992 *Appl. Phys. Lett.* **61** 3059
[9] Childress J R and Chien C L 1991 *Phys. Rev.* B **43** 8089
[10] Li Z G, Wan H, Liu J, Tsoukatos A, Hadjipanayis G C and Liang L 1993 *Appl. Phys. Lett.* **63** 3011
[11] Sang H, Jiang Z S, Guo G, Ji J T, Zhang S Y and Du Y W 1995 *J. Magn. Magn. Mater.* **140** 589
[12] Dieny B, Teixeira S R, Rodmacq B, Cowache C, Auffret S, Redon O and Pierre J 1994 *J. Magn. Magn. Mater.* **130** 197